FINITE ELEMENT SIMULATION OF BIPHASIC SOFT TISSUE CONTACT WITH APPLICATION TO THE SHOULDER JOINT

Kerem Ün, Robert L. Spilker
Department of Biomedical Engineering
Rensselaer Polytechnic Institute, Troy, NY, USA

Abstract - **We describe a method to simulate cartilage contact in diarthrodial joints such as the hip, knee and shoulder. The method derives time-dependent contact boundary conditions using kinematic, kinetic and geometric data that is collected experimentally and utilized to define the finite element (FE) analysis. The nonlinearity associated with contact is approximated using a penetration-based method, thus reducing the nonlinear problem to two linear ones, and greatly reducing the computational resources necessary. The method is applied to four shoulder models, allowing comparison of results that may be related to joint degeneration are compared.**
Keywords - **Cartilage, finite element, shoulder, orthopaedic biomechanics**

I. INTRODUCTION

Biomechanics involving the application of mechanics to the biological sciences has emerged as an critical branch of biomedical engineering. Soft tissues fulfill a wide range of functions in mammalian physiology. Soft tissue biomechanics is rapidly informing the study of organs as diverse as skin, brain, heart, tendons and cartilage. Mechanical properties of the soft tissue play an important role in function and determine the reaction of the tissue to mechanical effects.

Articular cartilage is a thin layer of soft tissue that covers the contacting portions of bones in diarthrodial joints, and carries the high contact forces [1] occurring during daily activities. Although it has remarkable durability, cartilage may be damaged by trauma or inflammatory disease, or may undergo progressive degeneration causing the clinical syndrome of osteoarthritis (OA).

This paper describes a method to simulate the mechanical response of cartilage to loading during physiological joint motion*. Our objective is to contribute to the understanding of mechanical factors in OA initiation, leading to the development of improved implant materials and artificial cartilage. We use kinematic data obtained experimentally from visualization techniques like magnetic resonance imaging (MRI) to derive time-dependent contact boundary conditions. These boundary conditions are used, together with a finite element (FE) analysis code, to simulate the joint motion. As an illustration, the method is applied to four physiological shoulder models.

II. GOVERNING EQUATIONS

The cartilage is modeled as biphasic, consisting of two distinct phases, the solid matrix and the interstitial fluid that fills the matrix. The interstitial fluid accounts for 70-80% of the cartilage volume, and is an important factor in the load bearing mechanism. Mow *et al.* [2] first considered the fluid phase when deriving the constitutive equations to form the biphasic theory of cartilage. Physically, the drag created by the movement of the fluid through the solid matrix gives the tissue its viscoelastic properties (although intrinsic matrix viscoelasticity can also be added [3]).

Assuming intrinsically incompressible phases, the mixture continuity, and the momentum equations of each phase are given by

$$\nabla \cdot \left(\phi^f \boldsymbol{v}^f + \phi^s \boldsymbol{v}^s\right) = 0, \tag{1}$$

$$\nabla \cdot \boldsymbol{\sigma}^\alpha + \boldsymbol{\Pi}^\alpha = \boldsymbol{0}, \ \alpha = s, f, \tag{2}$$

where s and f denote the solid and fluid phase, respectively. $\boldsymbol{v}^s$ refers to the velocity, while ϕ is phase fraction, $\boldsymbol{\sigma}$ stress and $\boldsymbol{\Pi}$ momentum exchange. Assuming an inviscid fluid phase, the constitutive equations are given by

$$\boldsymbol{\sigma}^s = -\phi^s p\boldsymbol{I} + \boldsymbol{\sigma}^E, \tag{3}$$

$$\boldsymbol{\sigma}^f = -\phi^f p\boldsymbol{I}, \tag{4}$$

$$\boldsymbol{\Pi}^s = -\boldsymbol{\Pi}^f = p\nabla\phi^s + K\left(\boldsymbol{v}^f - \boldsymbol{v}^s\right), \tag{5}$$

where p denotes the pressure and $\boldsymbol{K}$ the diffusive drag coefficient, which is related to permeability $\boldsymbol{\kappa}$ through $\boldsymbol{K} = (\phi^f)^2\boldsymbol{\kappa}^{-1}$, $\boldsymbol{\sigma}^E$ is the elastic stress tensor of the solid phase which, for a linear elastic material, can be written as

$$\boldsymbol{\sigma}^E = \mathbf{C}:\boldsymbol{\varepsilon}^s, \tag{6}$$

where $\boldsymbol{\varepsilon}^s$ is the strain tensor and $\mathbf{C}$ is the stiffness tensor. The total stress, $\boldsymbol{\sigma}^{Tot}$ is the sum of the phase stresses, ie.,

$$\boldsymbol{\sigma}^{Tot} = \boldsymbol{\sigma}^s + \boldsymbol{\sigma}^f = -p\boldsymbol{I} + \boldsymbol{\sigma}^E. \tag{7}$$

We manipulate (1-5) to eliminate the fluid terms, reducing the problem to two governing equations:

$$\nabla \cdot (\boldsymbol{\sigma}^E - p\mathbf{I}) = \boldsymbol{0}, \tag{8}$$

$$\nabla \cdot (\boldsymbol{v}^s - \boldsymbol{\kappa}\nabla p) = 0, \tag{9}$$

where $\boldsymbol{v}^s$ and p are the primary field variables for the problem. (Note that $\boldsymbol{\sigma}^E$ is a function of $\boldsymbol{v}^s$.) The boundary conditions for these governing equations are:

$$\boldsymbol{u}^s = \bar{\boldsymbol{u}}^s \quad \text{on } \Gamma_u, \tag{10}$$

$$p = \bar{p} \quad \text{on } \Gamma_p, \tag{11}$$

$$\bar{\boldsymbol{Q}} = -\boldsymbol{\kappa}\nabla p \cdot \boldsymbol{n} \quad \text{on } \Gamma_Q, \tag{12}$$

$$\boldsymbol{\sigma}^{Tot} \cdot n = \bar{\boldsymbol{t}} \quad \text{on } \Gamma_t. \tag{13}$$

* This study is supported by NIH, NSF and the Surdna Foundation

where Γ_u, Γ_p, Γ_Q and Γ_t are the appropriate parts of the boundary domain and $\boldsymbol{n}$ is the surface normal.

III. Finite Element Model

The problem domain (the physiological cartilage geometry) is complex, hence the governing equations can be solved only with a numerical technique such as the FE method. The weak form of the FE method is derived by using a weighted residual approach, multiplying (8), (9), (12) and (13) by weighting functions, integrating the resulting expressions over the discretized domain (FE mesh) and summing them to obtain the total residual. The solution is approximated with the same function space as the weighting functions (Galerkin method) to produce a symmetric first order differential algebraic system:

$$\begin{bmatrix} \boldsymbol{0} & -\boldsymbol{A} \\ -\boldsymbol{A}^T & -\boldsymbol{B} \end{bmatrix} \begin{bmatrix} \boldsymbol{v}^{sn} \\ \boldsymbol{p}^{n} \end{bmatrix} + \begin{bmatrix} \boldsymbol{K} & \boldsymbol{0} \\ \boldsymbol{0} & \boldsymbol{0} \end{bmatrix} \begin{bmatrix} \boldsymbol{u}^{sn} \\ \boldsymbol{0} \end{bmatrix} = \begin{bmatrix} \boldsymbol{F}_t \\ \boldsymbol{F}_Q \end{bmatrix}, \quad (14)$$

where the superscript n denotes the nodal values of each quantity, so that $\boldsymbol{v}^{sn}$ and $\boldsymbol{p}^{n}$ are the vectors containing nodal values. Matrices $\boldsymbol{A}$, $\boldsymbol{B}$, and $\boldsymbol{K}$ originate from the solid-fluid coupling, fluid stiffness and solid stiffness, respectively. $\boldsymbol{F}_t$ and $\boldsymbol{F}_Q$ are force vectors related to (12) and (13).

Equation (14) is solved in time with a finite-difference method. We use a generalized trapezoidal approach, and thus solid displacement is related to solid velocity by,

$$\boldsymbol{u}_{i+1}^{sn} = \left(\omega \boldsymbol{v}_{i+1}^{sn} + (1-\omega)\boldsymbol{v}_{i}^{sn}\right)\Delta t + \boldsymbol{u}_{i}^{sn}, \quad (15)$$

where the subscript refers to the time-step number, ω is a time-integration parameter and Δt is the time-step size. Substituting (15) into (14) gives the following linear system.

$$\begin{bmatrix} \omega \Delta t \boldsymbol{K} & -\boldsymbol{A} \\ -\boldsymbol{A}^T & -\boldsymbol{B} \end{bmatrix} \begin{bmatrix} \boldsymbol{v}_{i+1}^{sn} \\ \boldsymbol{p}_{i+1}^{n} \end{bmatrix} = \begin{bmatrix} \boldsymbol{F}_t - \boldsymbol{K}(\boldsymbol{u}_i^{sn} + \boldsymbol{v}_i^{sn}(1-\omega)\Delta t) \\ \boldsymbol{F}_Q \end{bmatrix}. \quad (16)$$

First, the Dirichlet boundary conditions, (10) and (11) are imposed on this system, noting that (15) can be used to relate $\boldsymbol{u}^{sn}$ and $\boldsymbol{v}^{sn}$. The force vector is time-dependent, but the coefficient matrix does not change with time. Hence, the matrix is factored only once and the back/forward substitutions are performed for each right hand side vector at each time step. The solution at the current time step is used to update the right hand side in preparation for the solution of the next time step.

IV. Penetration Method

The mechanical behavior of diarthrodial joints is dictated by contact, as forces are transmitted across the joint through the soft tissue layers, but analysis of 3-D biphasic contact is complicated and computationally demanding. In an effort to identify a computationally efficient method, in advance of full 3-D biphasic contact, we developed the penetration method to approximate soft tissue contact mechanics. The method reduces the problem of two biphasic tissues in contact over an unknown area to two problems, each with prescribed traction distributions over a pre-calculated (and therefore known) contact area. This replaces the non-linearity of contact analysis with a geometry-dependent preprocessing step. The nature of the contact of cartilage layers is characterized by how the load is split between the solid and fluid phases in the contact region. From (7) it is possible to write (in indical notation):

$$p = \sigma_{ij}^{E} n_i n_j - \sigma_{ij}^{Tot} n_i n_j \quad (17)$$

Equation (17) indicates that load splitting can be determined if any two of the three stress/pressure quantities can be calculated. The aim of the penetration method is to derive these quantities, determine the contact area, and satisfy the contact boundary conditions. In frictionless biphasic contact, the pressure and normal elastic traction at the contact interface should satisfy the following boundary conditions:

$$p^A - p^B = 0, \quad (18)$$

$$\sigma_{ij}^{E^A} n_i^A n_j^A - \sigma_{ij}^{E^B} n_i^B n_j^B = 0. \quad (19)$$

Input data for the penetration method originates from *in vivo* or *in vitro* joint experiments. The measurements include deformed and undeformed geometry of the cartilage layers, joint kinematics, and total joint loads. Since subchondral bone has a high modulus relative to cartilage we approximate it as a rigid body. Experimentally measured joint kinematics can therefore be specified at the interface between the subchondral bone and the articular cartilage layers. Applying the physiological joint kinematics to the initially undeformed cartilage models causes them to overlap in their physiological position (Fig. 1). At each contact point, we assume that the tissue deforms perpendicular to the contact surface, and that the total vector-valued penetration, $\boldsymbol{g}^{Tot}$, can be treated as the actual

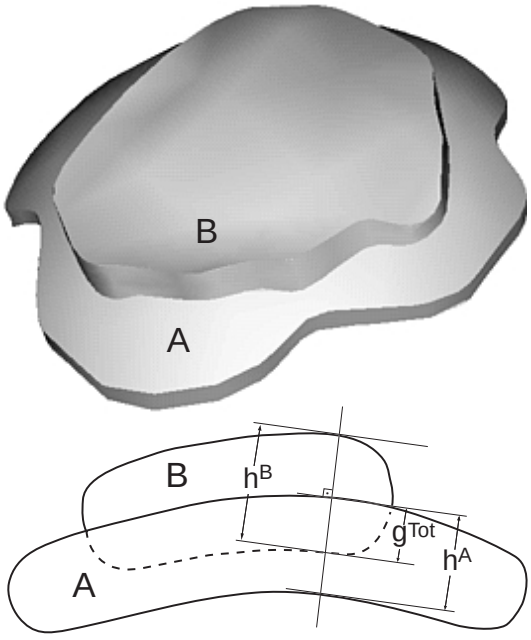

Fig 1. Penetrating undeformed models obtained from experimental data (top). A cross sectional view through the models and definition of quantities used in the penetration method at a contact point (bottom)

tissue deformation. At each contact point, we define a tangent-normal coordinate system where the only nonzero penetration component is the normal one denoted by the subscript n. That way we can directly manipulate the penetration magnitudes and write

$$u_n^{s^A} + u_n^{s^B} = u_n^{s^T} = g_n^{Tot} \tag{20}$$

The portion of the penetration associated with each tissue can be written as

$$u_n^{s^A} = g_n^A = \eta g_n^{Tot} \tag{21}$$

$$u_n^{s^B} = g_n^B = (1-\eta) g_n^{Tot} \tag{22}$$

where the superscripts A and B identify quantities associated with tissues A and B, respectively, and η is the splitting parameter. Available FE [4] and analytical solutions [5] suggest that the pressure is relatively uniform through the thickness of the tissue. Hence, according to (9), we expect the normal strain to be reasonably uniform and can be approximated as

$$\varepsilon_{nn}^{s^A} = \delta h^A / h^A = g_n^A / h^A \tag{23}$$

Note that the tangential strains contribute negligibly to the normal traction and are therefore neglected. In order to satisfy (19), the splitting parameter is given as

$$\eta = = 1 \Big/ \left(1 + {H^A h^B}/{H^B h^A}\right) \tag{24}$$

The penetration sharing between layers depends thus on H^A and H^B, the layer aggregate moduli (originating from $\mathbf{C}$.), and h^A and h^B, the layer thicknesses, both of which may vary *in-vivo*. Once the penetration is split, the quantity $\sigma^E_{ij} n_i n_j$ can be approximated using (23) and the tissue modulus.

The traction distribution is also equilibrated with the experimentally measured total joint force. Considering the load carrying mechanism of the tissue we assume that the total traction is proportional to the normal elastic strain which can be expressed as

$$\sigma_{ij}^{Tot} n_i n_j = \gamma^A \frac{g_n^A}{h^A} = \gamma^A \varepsilon_{nn}^A \tag{25}$$

where γ^A is the proportionality constant for layer A. The total contact traction, integrated component-wise over the contact surface, should be equal to the total force. Note that the force direction is determined by the penetration distribution, so we equate the magnitudes, i.e.

$$|\boldsymbol{F}|^2 = \sum_{i=1}^{3} F_i^2 = \sum_{i=1}^{3} \left(\gamma^A \int_{\Gamma^c} \frac{g_i^A}{h^A} d\Gamma^c \right)^2 \tag{26}$$

Since $|\boldsymbol{F}|$ is known, γ^A can be found and the quantity $\sigma^{Tot}_{ij} n_i n_j$ computed. Together with $\sigma^E_{ij} n_i n_j$, the information necessary to characterize the contact is thus known. The above procedure is repeated for layer B and gives independent boundary conditions for that layer. The pressure boundary condition is calculated according to (17) and applied during the FE analysis.

In exact biphasic contact, the solution has a run-time dependency on the geometry and modulus of the contacting layers. As shown, the penetration method converts this run-time solution dependency to a preprocessing dependency, and replaces intrinsically iterative biphasic contact analysis with non-iterative biphasic analysis of the individual layers. Although an approximation, the results of the penetration method have been shown in canonical contact problems [6] to satisfy (18) and (19), consistent with the requirements of biphasic contact.

V. Shoulder Example

OA consists of generally progressive loss of cartilage accompanied by repair and remodeling. In most cases, OA develops without any known cause, a condition referred as primary OA. Secondary OA, on the other hand, develops as a result of infection, injury or due to hereditary, metabolic, or developmental effects [7]. Pathological conditions leading to joint incongruity and asymmetric loading, such as fracture, surgical procedure, or disease, are listed among the causes of secondary OA. In addition, incongruity, asymmetric and nonuniform loading patterns can occur naturally in the joint without any pathological condition. To demonstrate this, we analyze four cadaveric, physiologically healthy shoulder joints using the penetration-based analysis. These joints are considered geometrically normal in terms of the thickness and congruity of their cartilage layers.

Typical shoulder joint tissue layers are shown in the top portion of Fig. 1. The larger tissue, humeral cartilage, covers the proximal end of the humerus bone. The smaller tissue, the glenoid, is attached to the scapula. Geometry, material properties, and joint kinematic data for these shoulder joints have been provided by the Orthopaedic Research Laboratory at Columbia University [8]. Solid models are formed from this geometrical data using the software *Parasolid*. The kinematic data corresponds to a coronal arm elevation motion from an angle of 30˚ to 150˚.

Using the penetration method, we derive moving contact boundary conditions at discrete elevation angles and interpolate through these over time to capture the smooth, time-dependent motion. The full range of motion takes place in 0.3 seconds, which is within physiological limits.

VI. Results

Penetration-based analysis showed similarities and differences in the mechanical response of the four normal shoulders. Two quantities, maximum tensile stress on the contact surface and maximum shear stress at the cartilage bone interface, are thought by some investigators to be related to cartilage damage. Our results indicate that both of these stress quantities behave similarly, hence our observations are applicable to both stress components. The analyses showed that glenoid cartilage experiences generally higher stresses than the humeral cartilage. The physiological locations of the high stresses on the glenoid at three elevation angles are given in Table 1. There is no regular pattern in high stress locations in the glenoid. We

observed that the glenoid of model 3, which experiences the lowest stresses, possesses a more symmetrical loading pattern. The glenoid of model 1 is loaded asymmetrically and thus experiences high stresses.

The maximum tensile stress on the contact face of each of the four humeral tissues is shown in Fig. 2 at an elevation angle of 70˚. The stress patterns give insight about the contact of the humeral cartilage with the glenoid cartilage. We notice that the asymmetry of the contact imprint on the humerus of model 1 is consistent with the load patterns we observed in the glenoid of the same joint. Similarly the load distribution is relatively uniform on the humerus of model 3 as expected. The shape and location of the contact imprint varies although the joints are in the same anatomical position.

VII. SUMMARY AND CONCLUDING REMARKS

In this work we described a method for simulation of cartilage layers in contact based on the processing of experimental data and the FE method. The method is computationally efficient compared with full 3-D FE contact analysis, and can be extended to account for large deformations, known to occur *in vivo*. In general, numerical joint simulation is an integral part of joint evaluation.

TABLE 1.
HIGH STRESS REGIONS ON THE GLENOID AT DIFFERENT CORONAL ARM ELEVATION ANGLES. S: SUPERIOR, I : INFERIOR, A : ANTERIOR, P : POSTERIOR.

Model	30˚	70˚	110˚
1	S, I, A	S, I, A	S, P
2	S, P	S, P	S, I
3	I,P	S,I,P	I,A,P
4	I	S, A	I, A

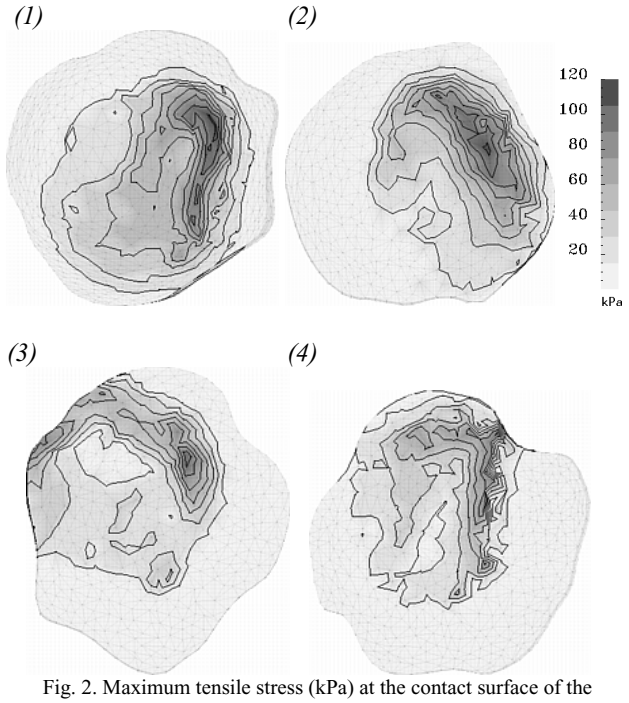

Fig. 2. Maximum tensile stress (kPa) at the contact surface of the humeral tissue in the four shoulders at 70˚ arm elevation.

Quantities that are difficult to measure experimentally can be obtained in a numerical simulation. For example, stress at the bone-tissue interface is such a quantity, and may have clinical significance with respect to cartilage failure.

In the present study, the method is used to analyze four normal adult cadaveric shoulder joints during coronal arm elevation. Our analyses indicate that each joint has a unique loading pattern. Different levels of asymmetric loading are observed in three models, while the fourth is more symmetric. We also obtained some quantitative values of the stress level likely to occur in the shoulder joint.

The penetration method can be especially powerful when used with nondestructive imaging techniques such as MRI. In that case patient specific data can be analyzed towards identifying high stress locations and evaluating the mechanical risk factors in the joint.

ACKNOWLEDGMENTS

The model data and clinical insights provided by the Columbia University Orthopaedic Research Laboratory, are gratefully acknowledged.

REFERENCES

[1]K. An, E. Y. S. Chao and K. R. Kaufman, “Analysis of muscle and joint loads”, in *Basic Orthopaedic Biomechanics*, V. C. Mow and W. C. Hayes eds., Lippincott-Raven, Philadelphia, 1997, pp. 1-37

[2]V. C. Mow, S. C. Kuei, W. M. Lai and C. G. Armstrong, “Biphasic creep and stress relaxation of articular cartilage in compression: theory and experiments”, *J. Biomech. Engng.*, vol. 102, 1980, pp. 73-84.

[3]A. F. Mak, “The apparent viscoelastic behavior of articular cartilage-The contributions from the intrinsic matrix viscoelasticity and interstitial fluid flows”, *J. Biomech. Engng.*, vol. 108, 1986, pp. 123-130.

[4]P. S. Donzelli and R. L. Spilker, “A contact finite element formulation for biological soft hydrated tissues”, *Comp. Meth. Appl. Mech. Engng.*, vol. 153, 1998, pp. 63-79.

[5]G. A. Ateshian, W. M. Lai, W. B. Zhu and V. C. Mow, “An asymptotic solution for the contact of two biphasic cartilage layers”, *J. Biomech.*, vol. 27, 1994, pp. 1347-1360.

[6]W. Dunbar, K. Ün, P. Donzelli and R. Spilker, “An evaluation of three dimensional diarthrodial joint contact using penetration data and the finite element method”, *J. Biomech. Engng.*, vol. (in press), 2001,

[7]H. J. Mankin, V. C. Mow and J. A. Buckwalter, “Articular cartilage repair and osteoarthritis”, in *Orthopaedic Basic Science: Biology and Biomechanics of the Musculoskeletal System*, American Academy of Orthopaedic Surgeons, 2000,

[8]V. M. Wang, V. C. Mow, R. A. Riamondo and E. L. Flatow, “The effects of rotator cuff tears and the long head of the biceps on glenohumeral kinematics”, in *1996 Advances in Bioengineering*, S. Rastegar, Editor 1996, ASME, pp. 175-176.